Understanding and Revisiting Properties of EuTiO_{3} Bulk Material and Films from First Principles

Yurong Yang, Wei Ren, Dawei Wang, and L. Bellaiche

Phys. Rev. Lett. **109**, 267602 — Published 26 December 2012

DOI: 10.1103/PhysRevLett.109.267602

Understanding and Revisiting Properties of $EuTiO_3$ Bulks and Films from First Principles

Yurong Yang,[1,2] Wei Ren,[1,3] Dawei Wang,[4] and L. Bellaiche[1]

[1]*Physics Department and Institute for Nanoscience and Engineering, University of Arkansas, Fayetteville, Arkansas 72701, USA*

[2]*Physics Department, Nanjing University of Aeronautics and Astronautics, Nanjing 210016, China*

[3]*Department of Physics, Shanghai University, 99 Shangda Road, Shanghai 200444, China*

[4]*Electronic Materials Research Laboratory, Key Laboratory of the Ministry of Education and International Center for Dielectric Research, Xi'an Jiaotong University, Xi'an 710049, China*

Abstract

Ab-initio computations are performed to investigate properties of bulks and epitaxial films made of $EuTiO_3$ (ETO). A whole family of nanoscale twinned phases, that present complex oxygen octahedra tilting (OOT) and unusual antiferroelectricity, is found to be degenerate in energy with simpler phases (all possessing typical antiphase OOT) in ETO *bulks*. Such degeneracy provides a successful explanation of recently observed anomalous phenomena. The calculations also lead to revisiting the (rich) phase diagram of ETO films.

The search for novel multiferroics [1] constitutes an important research direction, which explains why $EuTiO_3$ (ETO) systems have been recently investigated ([2–14]. One interesting finding in these materials is that, while ETO *bulk* is not multiferroic (it exhibits a G-type antiferromagnetic (AFM) ordering below 5.3 K [15] but is paraelectric down to 0K [16, 17]), epitaxial ETO *films* become both ferroelectric (FE) and ferromagnetic (FM) for large enough misfit strain [2, 13]. A recent experiment [6] suggested that, in contrast to what was previously believed, the ground state of ETO bulk is not cubic, paraelectric $Pm\bar{3}m$ but rather is tetragonal $I4/mcm$, and therefore exhibits oxygen octhadra tilting (OOT). This same work [6] pointed out an unusual difference between short-range and average crystallographic structures. For instance, Rietveld experiments yield a value of $\simeq 3.5^\circ$ for the angle associated with OOT, while pair distribution function analysis gave a value more than two times bigger! First-principle calculations [5] confirmed the importance of OOT in ETO bulk, but did not address the enigma about difference in local and average structures. Another measurement [7] determined that the OOT further adopts an unusual modulation that not only extends over several unit cells but also for which the corresponding diffraction peaks change in intensity, position and broadness over a long time period! The reason behind such change is unknown. Anomalous antiferroelectric patterns were further found to coexist with these modulated OOT [7]. One would like to know what is the real ground of ETO bulk and better understand this puzzling modulated OOT structure and its associated antiferroelectricity. Furthermore, all the previous experimental and theoretical studies on ETO *films* have overlooked OOT. As a result, their phase diagrams may need to be revisited.

This Letter resolves the aforementioned issues by conducting first-principles calculations. It explains the puzzling observations made in ETO bulk, based on a presently discovered degeneracy between "simple" OOT phases and a whole family of nanoscale twinned phases. This Letter also reports the existence of several novel equilibrium phases in ETO films.

Computations on $EuTiO_3$ systems are performed within density-functional theory (with an energy cutoff of 550 eV), as implemented in the Vienna ab initio simulation package (VASP) [18, 19]. Supercells containing 10, 20, 40, 60 or 80 atoms are used, with different Γ-centered k-point meshes (varying between $6 \times 6 \times 6$ and $6 \times 6 \times 1$), depending on the investigated phase. Both G-type AFM and FM orders are considered. More details about the method are given in the Supplemental Material [20–26].

Let us first focus on ETO *bulk*, by allowing the cell shape and volume of the supercells

mimicking different phases to fully relax. We investigated the following states with different OOT patterns (indicated by Glazer's notations [27]): cubic $Pm\bar{3}m$ ($a^0a^0a^0$), tetragonal $P4/mbm$ ($a^0a^0c^+$), orthorhombic $Pnma$ ($a^-a^-c^+$), tetragonal $I4/mcm$ ($a^0a^0c^-$), orthorhombic $Imma$ ($a^-a^-c^0$), rhombohedral $R\bar{3}c$ ($a^-a^-a^-$) and monoclinic $C/2c$ ($a^-a^-c^-$). A 20-atom supercell is used for all these states. A G-type antiferromagnetism is adopted, since we found it to be of lower energy than FM order. Out of these phases, four of them are energetically much more stable than $Pm\bar{3}m$: the $I4/mcm$, $Imma$, $Pnma$ and $C2/c$ states are lower in energy by 37, 36, 36 and 35 meV per 5 atom, respectively. Such results are consistent with those of Ref. [5], and therefore emphasize the need of incorporating OOT (also, termed antiferrodistortive, AFD, motions) to properly describe ETO systems [28]. They also further confirm that different "simple" states have very similar energy and that $I4/mcm$ is the lowest of them by a minute amount – as also in agreement with Ref. [5].

Let us now determine if states with higher complexity can also be of low energy in ETO bulk. We have in mind to consider complex oxygen octahedra tilting about the [001] pseudo-cubic direction. Examples include "mmpp", "mmpppp", "ppppmmmm" patterns that repeat themselves periodically along a line being parallel to [001] and joining neighboring Ti atoms. Here, 'p' (respectively, 'm') denotes an O_6 oxygen octahedron rotating clockwise (respectively, counterclockwise) about [001]. Such nanoscale twinned phases have been proposed in $EuTiO_3$ bulk [7], based on X-ray data. We investigated several phases for which the tilting patterns can be described in a modified Glazer notation [27] by $a^0a^0c^m$ and $a^-a^-c^m$, where c^m corresponds to the aforementioned complex tilting about [001] (with a possible periodic length of 4, 6 and 8 unit cells), and where a^0 and a^- denote no tilting and anti-phase tilting, respectively, about the [100] and [010] pseudo-cubic directions, respectively. Table I of the Supplemental Material provides the total energy of such complex phases and compares them with that of the simple tilted $I4/mcm$ and $C2/c$ phases (indicated in the first row of that Table). One can see that several different $a^-a^-c^m$ phases (e.g., "mmpppp", "mmmppp", "ppppmmmm", "pppppmmm" and "ppppppmm") have energies that are nearly identical to that of the simplier $I4/mcm$ state. In other words, there is a whole family of nanoscale twinned phases whose energies are basically degenerate with that of the recently assumed $I4/mcm$ ground state [5, 6] of bulk ETO [29]! Such degeneracy likely implies that nanodomains formed by different phases can coexist in $EuTiO_3$ bulk, with the size of these domains (and resulting macrosocopic properties) having the possibility to

evolve with time – as in non-ergodic systems [30]. Such degeneracy therefore provides a successful explanation for some striking phenomena observed in Refs. [6, 7], such as the change in intensity, position and broadness of diffractions peaks over a long time period or the mismatch between short-range and average crystallographic structures. For instance, it is remarkable that (i) the tilt angle of $\simeq 3.5^\circ$ measured from Rietveld measurement in Ref. [6] nearly coincides with our prediction that the amplitude of the different oxygen octahedral tilts about [001] in all these low-energy nanoscale twinned phases are of the order of 3° [31]; and (ii) that the same experimental study [6] extracted a much larger tilt angle of 8° from (short-range) pair distribution function analysis, while we numerically found that the antiphase tilting angle about [001] in the more simple $I4/mcm$ state is indeed around 8°. Items (i) and (ii) suggest that nanodomains made of $I4/mcm$ and of the more complex twinned AFD phases are both present in ETO bulks. The nanoscale twinned phases are also found to have unusual antiferroelectricity. For instance, the state possessing a "mmmppp" tilting pattern about [001] and antiphase octahedral tiling about [110] exhibits antiferroelectric displacements for the Eu ions of the type "-+0-+0" when moving along adjacent (001) planes and where '-' and '+' represent displacement along $[\bar{1}\bar{1}0]$ and [110], respectively, while '0' represents zero displacement. Such antiferroelectricity is therefore associated with a k-vector that lies in-between the Γ and X-points of the cubic first Brillouin zone. Strikingly, Ref. [7] also invoked unusual antiferroelectric displacements that are consistent with such kind of k-point to explain weak intensities in the X-ray spectra of nanoscale twinned tilting phases of ETO bulk. However, antiferroelectricity in Ref. [7] was assumed to be caused by Ti atoms moving along [001] or $[00\bar{1}]$ directions rather than by Eu atoms moving along $[\bar{1}\bar{1}0]$ and [110]. Our prediction of A-driven antiferroelectric, in-plane motions being coupled to out-of-plane complex oxygen octahedra tilt is fully consistent with what is documented in $BiFeO_3$ systems [32] and with symmetry [33]. We also report, in parenthesis in Table I of the Supplemental Material, the energies of the simple $a^-a^-c^-$ ($C2/c$) and $a^-a^-c^+$ ($Pnma$) states as well as the complex $a^-a^-c^m$ with c^m corresponding to the "mmmppp" pattern, *when the antiferroelectric displacements of Eu atoms are prevented from occurring* (symmetry implies that these motions can exist in the last two phases, but not in the $a^-a^-c^-$ state [32]). These energies as well as the relaxed ones for these three phases indicate that (1) a pure antiphase tilting about [001] ($a^-a^-c^-$ state) is intrinsically of lower energy than a pure in-phase tilting about this direction ($a^-a^-c^+$ state), but by a relatively small amount, of

the order of 0.9 meV, when Eu antiferroelectric motions are annihilated; (2) the complex tilting pattern has an intermediate energy between those of $a^-a^-c^-$ and $a^-a^-c^+$ when Eu antiferroelectric displacements are not incorporated; and (3) phases having in-phase tilting (such as $a^-a^-c^+$ and $a^-a^-c^m$) can even further decrease their energies via the occurrence of Eu antiferroelectric displacements. Items (1)-(3) therefore explain why nanoscale twinned phases can be of low energy in ETO.

Let us now shift our attention to ETO *films* that are epitaxially grown along [001]. Mimicking such films consists of imposing that (001) planes all have a square-basis lattice of parameter a_{IP}, with a_{IP} having the possibility to vary in order to model the growth of ETO films on different substrates. The misfit strain is defined as $\eta = \frac{a_{IP}-a_0}{a_0}$, where $a_0 = 3.87$ Å is the in-plane lattice constant found for the equilibrium $I4/mcm$ phase of ETO *bulk*.

Figure 1a shows the total energy of "simple" states of (001) ETO film for misfit strain ranging between -8% and 8% (note that the largest investigated strains are likely not achievable in experiments, but their associated structural phases may be found at smaller strains at finite temperature). Using FM or G-type AFM ordering provides similar curve for each of these phases in Fig. 1a because of the scale of this figure. To resolve this issue, the energy *difference* between FM and AFM for each of these crystallographic states is displayed in Fig. 1b as a function of misfit strain. Figures 2a and 2b show Cartesian components of the polarization (as calculated from the modern theory of polarization [34]) and of the *antiphase* antiferrodistortive (AAFD) vector, respectively, for some of these simple states – while the inset of Fig. 2b displays Cartesian components of the *in-phase* antiferrodistortive (IAFD) vector. Note that the AAFD (respectively, IAFD) vector is defined such that its axis provides the direction about which oxygen octahedra tilt in *antiphase* (respectively, *in-phase*), whereas its magnitude provides the angle of such tilting [35]. The x-, y- and z-axis are along the pseudo-cubic [100], [010] and [001] directions, respectively. Figures 1a and 1b also report the strain dependence of the total energy and of the difference in energy between FM and G-type FM states for a particular nanoscale twinned phase. This phase is the one shown in the inset of Fig. 1a, and possesses a periodic "mmmppp" tilting pattern along [001] as well as "regular" antiphase octahedral tiling about [110].

Let us first focus on compressive strains. Figs. 1 indicate that, for η ranging between 0 and -3%, ETO films adopt a tetragonal $I4/mcm$ state, with a G-type AFM ordering between Eu atoms, as its ground state. Such state is paraelectric. On the other hand, this $I4/mcm$

phase possesses a non-vanishing z-component of its AAFD vector that increases from $\sim 8^\circ$ to $\sim 11^\circ$ when strengthening the strain from 0 to -3% (see Fig. 2b). At $\eta = -3\%$, the epitaxial (001) ETO film then undergoes a second-order phase transition from this $I4/mcm$ phase to a $I4cm$ state, which is characterized by the appearance of an out-of-plane component of polarization in addition to the preexisting out-of-plane component of the AAFD vector. Both of these out-of-plane components increase as the magnitude of compressive strain increases from 3% to 5.4%. Strikingly, the $I4cm$ phase adopts an AFM ordering for η ranging between -3% to -3.8%, while it is FM for larger-in-magnitude compressive strain. Moreover, at $\eta = -5.4\%$, a first-order strain-driven phase transition from this tetragonal FM $I4cm$ phase to a tetragonal FM $P4mm$ phase occurs. In this $P4mm$ state, the AAFD vector is annihilated while the z-component of the polarization is large and further increases when the magnitude of compressive strain increases from 5.4% to $\simeq 7\%$. Some of our results qualitatively agree with those of Ref. [13], namely that (001) ETO films are paraelectric and AFM at small compressive strains while being FE and FM at larger compressive strain. However, we predict the magnetic transition to occur at around -3.8% while a critical value of $\simeq -1\%$ is provided in Ref. [13]. Moreover, unlike in Ref. [13], our computations point out that the strain-induced change between AFM and FM order happens within the *same* phase (namely, $I4cm$). Such differences between our study and the pioneering work of Ref. [13] is due to our incorporation of AFD motions.

Let us now turn our attention to (001) ETO films under *tensile strain*. Figs. 1a and 1b reveal that, when $0.25\% < \eta < 1.9\%$, the "simple" orthorhombic $Imma$, $Pnma$ and monoclinic $C2/c$ phases, as well as the "mmmppp" twinned phase (1) have total energies that are not only lower than that of $I4/mcm$ but are also basically equal to each other; and (2) all adopt a G-type AFM order. The $Imma$ state possesses a significant in-plane, strain-independent AAFD vector, for which the x and y components are equal to each other and are $\simeq 6.2^\circ$. The "simple" $C2/c$ state has both in-plane and out-of-plane components of the AAFD vector. The x and y components of this vector are identical and equal to 4.5° at 0.25% tensile strain, and slightly increases with η. On the other hand, the out-of-plane component of the AAFD vector is about 5.5° and decreases with the tensile strain. Moreover, the $Pnma$ state possesses in-plane components of the AAFD vector of about 6° and an out-of-plane component of the IAFD vector of 2.5° in this strain region. We also numerically found (not shown here) that, in the "mmmppp" nanoscale twinned phase, the

antiphase octahedral tiling about [110] are quantitatively unchanged, while the local angle in the complex tilting pattern about [001] decreases from $\sim 3^\circ$ to $\sim 2^\circ$ and the antiferroelectric displacements grows when increasing the tensile strain from 0.25% to 1.9%.

For η ranging between 1.9% and 6.5%, the ground state of (001) epitaxial ETO films becomes orthorhombic $Ima2$ and is now FM. It exhibits a polarization aligned along the in-plane [110] direction that increases in magnitude as the strain increases from +1.9% to +6.5%. Our calculations thus reproduce previous results [2] that a large-enough tensile strain can induce a phase that is FE and FM while (001) ETO films under very small strain are paraelectric and AFM. However, unlike what was proposed in Ref. [2], the resulting strain-induced FE and FM structure is not $Amm2$. It is rather $Ima2$ since it also exhibits antiphase oxygen octahedra tilting about the in-plane [110] direction [36].

At the tensile strain of 6.5 %, (001) ETO films undergo a first-order phase transition from $Ima2$ to a state of $Pmc2_1$ symmetry. Such state has also been found in $BiFeO_3$ and $PbTiO_3$ films [37]. As in $Ima2$, it possesses an in-plane polarization along [110] and is FM. However, unlike $Ima2$, the $Pmc2_1$ state has a vanishing AAFD vector while exhibiting OOT being *in-phase* about the z-axis. The resulting tilting angle has a magnitude of $\simeq 8^\circ$ near the transition, that further increases with the tensile strain. We also found (not shown here) that $Pmc2_1$ has in-plane, zig-zag pattern for the Eu (or Ti) atoms belonging to any (001) plane [37], and exhibits *orbital ordering* between *f-electron* of Eu atoms.

In summary, this work provides a successful explanation for observed anomalies in ETO bulk (via the existence of a family of degenerate, nanoscale twinned phases), and revisits the phase diagram of epitaxial ETO films. Interestingly, nanoscale twinned phases have been observed in $NaNbO_3$ [38–41], $AgNbO_3$ [42], and $CaSrTiO_3$ [43], and have also been predicted in $BiFeO_3$-based systems [32]. It is also likely plausible that they can explain unusual phenomena that have been reported in the $(Na,Bi)TiO_3$ and $(Na,Bi)TiO_3$-$BaTiO_3$ lead-free materials [44]. These complex twinned phases may thus constitute a general but typically overlooked feature of perovskites.

The authors thank Dr. S. Prosandeev and Dr. J. Íñiguez for useful discussions. This work is mostly supported by the Department of Energy, Office of Basic Energy Sciences, under contract ER-46612. We also acknowledge ARO Grant W911NF-12-1-0085, ONR Grants N00014-11-1-0384 and N00014-08-1-0915, and NSF grants DMR-1066158 and DMR-0701558 for discussions with scientists supported by these grants. Some computations were

also made possible thanks to the MRI grant 0722625 from NSF, the ONR grant N00014-07-1-0825 (DURIP) and a Challenge grant from the Department of Defense.

---

[1] Y. Wang, J. Hu, Y. Lin, and C.-W. Nan, *NPG Asia Mater.* **2**, 61 (2010).

[2] J. H. Lee, L. Fang, E. Vlahos, *et al.*, *Nature* **466**, 954 (2010).

[3] T. Katsufuji and H. Takagi, *Phys. Rev. B* **64**, 054415 (2001).

[4] Q. Jiang and H. Wu, *J. Appl. Phys.* **93**, 2121 (2003).

[5] K. Z. Rushchanskii, N. A. Spaldin, and M. Ležaić, *Phys. Rev. B* **85**, 104109 (2012).

[6] M. Allieta, M. Scavini, L. J. Spalek, *et al.*, *Phys. Rev. B* **85**, 184107 (2012).

[7] J.-W. Kim, P. Thompson, S. Brown, *et al.*, (2012), arXiv:1206.5417v1.

[8] K. Fujita, N. Wakasugi, S. Murai, *et al.*, *Appl. Phys. Lett.* **94**, 062512 (2009).

[9] H.-H. Wang, A. Fleet, J. D. Brock, *et al.*, *J. Appl. Phys.* **96**, 5324 (2004).

[10] J. H. Lee, X. Ke, N. J. Podraza, *et al.*, *Appl. Phys. Lett.* **94**, 212509 (2009).

[11] K. Kugimiya, K. Fujita, K. Tanaka, and K. Hirao, *J. Magn. Magn. Mater.* **310**, 2268 (2007).

[12] S. Kamba, V. Goian, M. Orlita, *et al.*, *Phys. Rev. B* **85**, 094435 (2012).

[13] C. J. Fennie and K. M. Rabe, *Phys. Rev. Lett.* **97**, 267602 (2006).

[14] A. Bussmann-Holder, J. Köhler, R. K. Kremer, and J. M. Law, *Phys. Rev. B* **83**, 212102 (2011).

[15] G. McCarthy, W. White, and R. Roy, *J. Inorg. Nucl. Chem.* **31**, 329 (1969).

[16] C.-L. Chien, S. DeBenedetti, and F. D. S. Barros, *Phys. Rev. B* **10**, 3913 (1974).

[17] T. R. McGuire, M. W. Shafer, R. J. Joenk, *et al.*, J. Appl. Phys. **37**, 981 (1966).

[18] G. Kresse and J. Hafner, *Phys. Rev. B* **47**, 558 (1993).

[19] G. Kresse and J. Furthmüller, *Phys. Rev. B* **54**, 11169 (1996).

[20] O. Diéguez, O. E. González-Vázquez, J. C. Wojdeł, and J. Íñiguez, *Phys. Rev. B* **83**, 094105 (2011).

[21] Y. Yang and L. Bellaiche, in 2012 *High Performance Computing Modernization Program Contributions to DoD Mission Success* (New Orleans, Louisiana, USA, 2012).

[22] J. P. Perdew, A. Ruzsinszky, G. I. Csonka, *et al.*, *Phys. Rev. Lett.* **100**, 136406 (2008).

[23] S. L. Dudarev, G. A. Botton, S. Y. Savrasov, *et al.*,*Phys. Rev. B* **57**, 1505 (1998).

[24] J. P. Perdew, K. Burke, and M. Ernzerhof, *Phys. Rev. Lett.* **77**, 3865 (1996).

[25] H. Akamatsu, Y. Kumagai, F. Oba, *et al.*, *Phys. Rev. B* **83**, 214421 (2011).

[26] G. Lawes and G. Srinivasan, *J. Phys. D: Appl. Phys.* **44**, 243001 (2011).

[27] A. Glazer, *Acta Crystallogr., Sect. B* **28**, 3384 (1972).

[28] We found that $R\bar{3}c$ transforms into $C2/c$ during the self-consistency procedure, which contrasts with the prediction of a stable $R\bar{3}c$ given in Ref. [5]. Such discrepancy may be due to the difference in exchange-correlation functionals used in this previous work and the present study.

[29] Nanoscale twinned phases with a periodicity along the z-axis being larger than 8 unit cells may also have similar energy than that of $I4/mcm$. Such states are likely those observed in Ref. [7], but are not considered here because they are associated with too large supercells.

[30] Igor A. Kornev and L. Bellaiche, *Phys. Rev. Lett.* **91**, 116103 (2003).

[31] The antiphase octahedral tiling about [110] is about 6-8° in all these low-energy nanoscale twinned phases for ETO bulk. Moreover, the different tilting angles about [001] are shown in the inset of Fig. 1a for the $a^-a^-c^m$ structure where c^m corresponds to the "mmmppp" pattern. They vary between 2.6 and 3.3 degrees.

[32] S. Prosandeev, D. Wang, W. Ren, *et al.*, *Adv. Func. Mater.* (2012); DOI: 10.1002/adfm.201201467.

[33] Note that we have built the complex structure proposed in Ref. [7] and relaxed it. After some relaxation steps, the Ti atoms moved back to their ideal positions and therefore the antiferroelectricity associated with Ti atoms vanishes.

[34] R. D. King-Smith and D. Vanderbilt, *Phys. Rev. B* **47**, 1651 (1993).

[35] Igor A. Kornev, L. Bellaiche, P.-E. Janolin, B. Dkhil and E. Suard, *Phys. Rev. Lett.* **97**, 157601 (2006).

[36] We thus predict that the ground state of (001) ETO films is FE and FM for strains equal or above +1.9% when choosing the zero strain as corresponding to the equilibrium in-plane lattice constant of $I4/mcm$. Such critical strain value becomes +1.1% if we use the equilibrium *cubic* lattice constant of 3.9 Å as reference for the zero strain.

[37] Y. Yang, W. Ren, M. Stengel, *et al.*, *Phys. Rev. Lett.* **109**, 057602 (2012).

[38] V. Shuvaeva, M. Antipin, S. Lindeman, *et al.*, *Sov. Phys. Crystallogr.* **37**, 814 (1992).

[39] V. Shanker, S. L. Samal, G. K. Pradhan, *et al.*, *Solid State Sci.* **11**, 562 (2009).

[40] K. E. Johnston, C. C. Tang, J. E. Parker, *et al.*, *J. Am. Chem. Soc.* **132**, 8732 (2010).

[41] M. D. Peel, S. P. Thompson, A. Daoud-Aladine, *et al.*, *Inorg. Chem.* **51**, 6876 (2012).

[42] M. Yashima, S. Matsuyama, R. Sano, *et al.*, *Chem. Mater.* **23**, 1643 (2011).

[43] C. J. Howard, R. L. Withers, K. S. Knight, and Z. Zhang, *J. Phys.: Condens. Matter* **20**, 135202 (2008).

[44] J. E. Daniels, W. Jo, J. Rodel, D. Rytz, and W. Donner, *Appl. Phys. Lett.* **98**, 252904 (2011).

FIGURE CAPTIONS

Figure 1: (Color online) Predicted total energy of the G-type AFM state (Panel a) and energy difference between the G-type AFM and FM states (Panel b) versus the misfit strain for low-in-energy phases in epitaxial (001) ETO films. The inset of Panel (a) displays a schematic of the $a^-a^-c^m$-type nanoscale twinned phases possessing the "mmmppp" tilting pattern. In this inset, the curled and straight arrows represent oxygen octahedra tilting about [001] or [00$\bar{1}$] and antiferroelectric Eu displacements, respectively. The different tilting angles about [001] are also provided here.

Figure 2: (Color online) Evolution of the polarization (Panel a) and AAFD vector (Panel b) with strain for equilibrium phases. The inset of Fig. 2b shows the IAFD vector of the $Pnma$ and $Pmc2_1$ state. Open symbols display the x component (which is identical to the y component) while solid symbols show the z component. For strain ranging between 0.25 and 1.9%, the rhombus, inverted triangles and triangles correspond to $Imma$, $Pnma$ and $C2/c$ states, respectively, in Panel b.

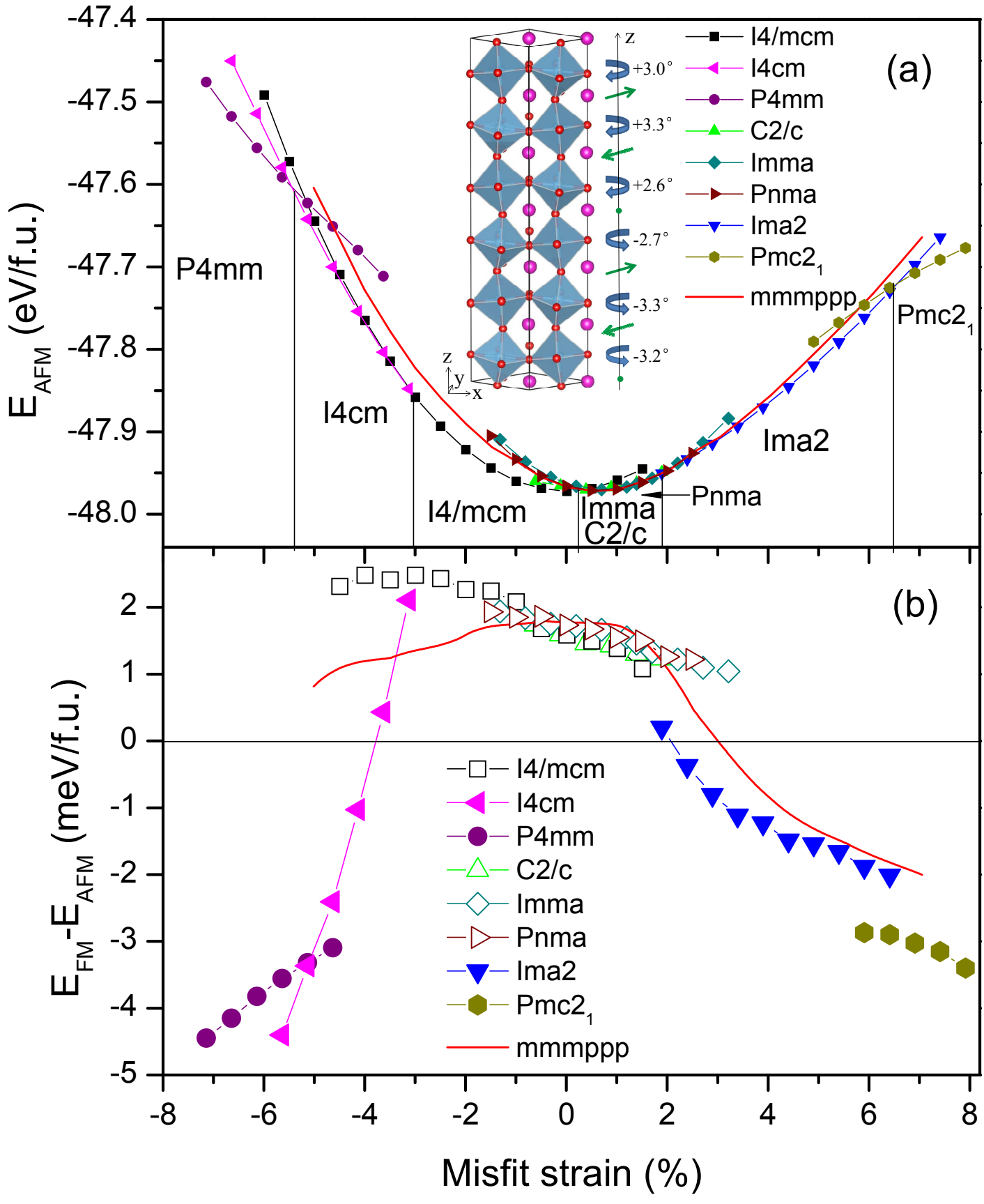

Figure 1 XXXXXXX 16Nov2012

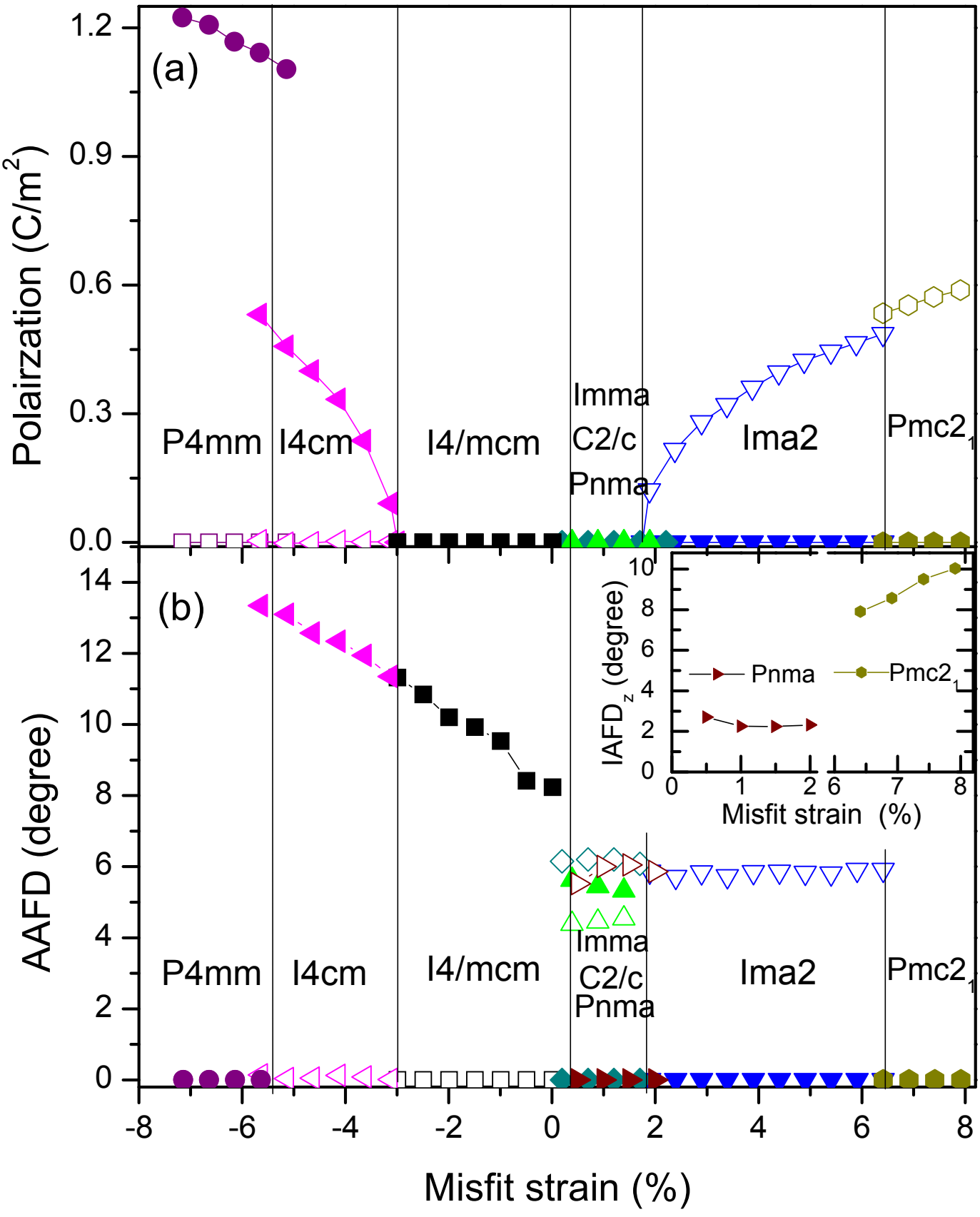

Figure 2 XXXXXXX 16Nov2012